Optical Coupling of Deep-Subwavelength Semiconductor Nanowires

ARTICLE *in* NANO LETTERS · MARCH 2011

Impact Factor: 13.59 · DOI: 10.1021/nl1040429 · Source: PubMed

3 AUTHORS, INCLUDING:

Pengyu Fan
Stanford University
11 PUBLICATIONS **710** CITATIONS
SEE PROFILE

Mark L Brongersma
Stanford University
272 PUBLICATIONS **12,135** CITATIONS
SEE PROFILE

NANO LETTERS

LETTER

pubs.acs.org/NanoLett

Optical Coupling of Deep-Subwavelength Semiconductor Nanowires

Linyou Cao, Pengyu Fan, and Mark L. Brongersma*

Geballe Laboratory for Advanced Materials, Stanford University, California 94305, United States

Supporting Information

ABSTRACT: Systems of coupled resonators manifest a myriad of exciting fundamental physical phenomena. Analogous to the synthesis of molecules from single atoms, the construction of photonic molecules from stand-alone optical resonators represents a powerful strategy to realize novel functionalities. The coupling of high quality factor (Q) dielectric and semiconductor microresonators is by now well-understood and chipscale applications are abound. The coupling behavior of low-Q nanometallic structures has also been exploited to realize high-performance plasmonic devices and metamaterials. Although dense arrays of semiconductor nanoparticles and nanowires (NWs) find increasing use in optoelectronic devices, their photonic coupling has remained largely unexplored. These high refractive index nano-objects can serve as low-Q optical antennas that can effectively receive and broadcast light. We demonstrate that the broad band antenna response of a pair of NWs can be tuned significantly by engineering their optical coupling and develop an intuitive coupled-mode theory to explain our observations.

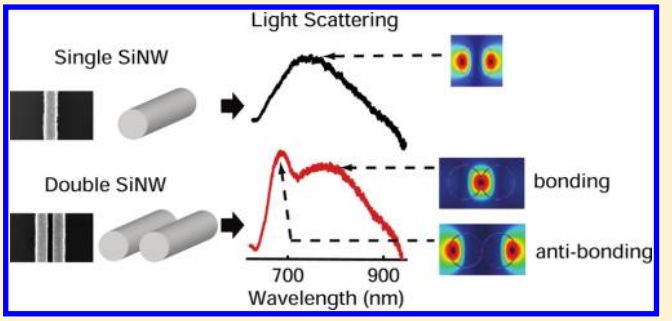

KEYWORDS: Nanowire, optical antenna, coupled mode theory, photonic molecule, nanophotonics

The behavior of complex physical systems is intimately related to the way in which constitutive building blocks are linked together. A two-body system provides the most elementary testbed for study of the fundamental interaction between individual units. Historically, study of the hydrogen (H_2) molecule revealed the rich nature of the chemical bond and played a key role in the development of quantum mechanics. Remarkably, the physics governing the optical coupling between photonic resonators bears great resemblance to the electronic coupling/bonding in molecules.[1−5] The optical interaction between two identical microcavities in a photonic "molecule" can cause degenerate optical states of individual resonators to be split into antibonding and bonding states with distinct eigenfrequencies.[3,4,6−8] Through the construction of systems consisting of a plurality of optical resonators, one can further enable a transformation of a set of discrete optical eigenfrequencies into continuous photonic bands.[7] This parallel between the behavior of electrons in molecules and photons in optical resonators suggests an intuitive vantage point from which to design complex optical systems.

A wealth of electromagnetic complex interactions between neighboring microscale dielectric and semiconductor optical resonators has been documented.[4,6−13] It enabled manifestation of many exciting functionalities that are not present in stand-alone resonators, including optical actuation,[4,8,14] lossless optics waveguiding,[9,15] and electromagnetic-induced transparency (EIT).[11] These interactions rely in essence on the exchange of photons between the resonators, much like the exchange of electrons between neighboring atoms in molecules. Despite the significant progress made with microscale systems, the increased demand for ultracompact optical devices and circuits has prompted for an improved understanding of the optical coupling between semiconductor nanoscale resonators; such structures have remained largely unexplored. Unlike the highly confined, high quality factor (Q) modes that can be found in microresonators, the optical modes supported by nanoscale versions are often very leaky (i.e., radiate efficiently) and thus low Q. Whereas such properties are undesirable for a number of traditional photonics applications, such as low threshold lasers and nonlinear devices, novel applications are also emerging. For example, new science is currently enabled with single nanoscale semiconductor structures that effectively interface with the outside world by serving as broad band optical antennas.[16] A deep understanding of the scaling characteristics of coupled optical resonators going from the superwavelength microscale to the subwavelength nanoscale allows for rational tuning of their resonant optical response. This in turn will enable new designs of various passive and active nanophotonic components consisting of a plurality of semiconductor nanostructures, including light sources, optical filters, switches, photodetectors, nanoscale versions of coupled resonator optical waveguides (nano-CROWs[15]), nanoscale antenna arrays, and metamaterials. This work nicely complements the large efforts on the development of equally low-Q, coupled nanometallic antennas for use in plasmonic devices and metamaterials.

In this paper, we demonstrate the leaky mode coupling between neighboring silicon nanowires (SiNWs). This is

Received: November 18, 2010
Revised: February 24, 2011
Published: March 28, 2011

dx.doi.org/10.1021/nl1040429 | *Nano Lett.* 2011, 11, 1463–1468

accomplished through an analysis of light scattering spectra taken from bi-NW structures consisting of two parallel NWs of similar diameter. High refractive index NWs can serve as optical waveguides or cavities through the excitation of their guided or leaky modes. Whereas the coupling of guided modes of semiconductor NWs has been the topic of much research,[3,14,17,18] the coupling between their leaky modes has not yet been explored. An individual NW can act as a nanoscale cylindrical cavity resonator when side-illuminated at a wavelength that matches one of its leaky modes. Intuitively, the strong, tunable leaky mode resonances (LMRs) in large diameter wires can be understood as resulting from constructive interference of the light trapped inside the NW that circulates along the periphery by multiple total internal reflections. As a result, a high refractive index NW can effectively trap, absorb, or scatter light at several resonant wavelengths.[16,19,20] With the latest advances in the semiconductor industry, such nanostructures can now be fabricated with atomic precision, and coupled NW systems thus offer an appealing new route to manipulate the flow of light at the nanoscale.

Coupled mode theory (CMT) has extensively been used to analyze the electromagnetic interactions between optical structures, and microresonators provide a beautiful example.[20] The principal feature of the CMT is that it treats composite structures as a collection of more elementary building blocks. In the composite, the modes associated with the individual building blocks are perturbed by the presence of the others. These perturbations lead to coupling and exchange of power among the various elements. For coupled resonators, CMT is typically formulated by considering the exchange of power between resonators and by requiring conservation of the total energy in the coupled system.[20] This approach leads to erroneous results for coupled nanostructures that support leaky modes (as energy can escape from this open system).[21] Here, we develop an alternative formulation that captures the physics underlying the leaky mode coupling of the NWs. This formulation is based in part on the CMT developed by Snyder to describe the interaction of guided modes of neighboring waveguides.[21] Similar to this model, we start from the scalar wave equation and write it down for a bi-NW structure as illustrated in Figure 1a. This equation is

$$(\nabla_t^2 + k^2 n^2(x,y) - \beta^2)E_t = 0$$

where $n(x,y)$ is the refractive index profile, β is the propagation constant along the z direction (the NW axis), t a subscript referring to the transverse directions perpendicular to the NW axis, and k the component of the wave vector in the transverse direction of the bi-NW. Whereas the use of CMT is typically aimed at obtaining the axial propagation constant β for coupled waveguides, our goal is to calculate the magnitude of the transverse wave vectors, k, for bi-NWs from the basic leaky modes of single NWs. For TM and transverse electric (TE) leaky modes with $\beta = 0$, the wave equation can be simplified to:

$$-\frac{1}{n^2(x,y)}\nabla_t^2 E_t = k^2 E_t \qquad (1)$$

This wave equation holds for each of the two individual NWs (NW 1 and NW 2) that we would like to couple together

$$-\nabla_t^2 E_{a,b}/n_{a,b}^2(x,y) = k_{a,b}^2 E_{a,b}$$

Here, we have omitted the subscript t with the field for convenience. With the approximation of weak coupling that has been extensively used in the conventional CMT,[20,21] the

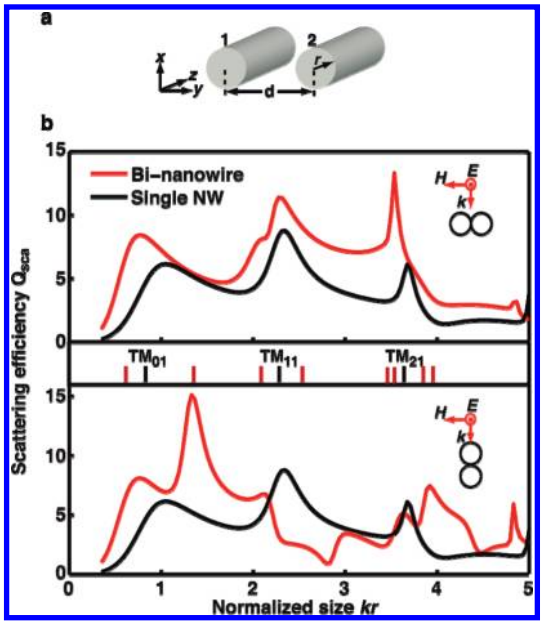

Figure 1. Theoretical model for the coupling of leaky modes. (a) Schematic illustration of the investigated binanowire (bi-NW) structures consisting of two parallel NWs with an identical radius, r, and a center-to-center distance, d. (b) Calculated spectral back scattering efficiency, Q_{sca}, of a single NW (black) and of bi-NWs (red) in the side-by-side (upper) overlap (lower) configuration. The TM-polarized, plane wave illumination conditions are shown in the insets. The refractive index was taken to be 3.5, the interspacing, d, was set to be $2r$ (the nanowires touch each other), and the results are plotted as a function of a normalized size nk_0r or kr, where k_0 is the wavenumber of the incident light. The ticks (middle panel) between the upper and lower panels indicate the predicted locations for the scattering resonances for single NW (black) and bi-NW (red) structures.

symmetry of the bi-NW resonators dictates that the two fundamental solutions of eq 1 can be written in terms of the fields of each well-separated nanowire (E_a and E_b). We find $E = E_a + E_b$ for symmetric modes and $E = E_a - E_b$ for antisymmetric modes.

We can now relate the eigenvalues k of the bi-NW system to those of the individual NWs. After multiplying both sides of eq 1, with the conjugated field, E_a^*(or E_b^*), integrating over the cross-sectional area of wire a (or b), and finally substituting the wave equations of the individual NWs to eliminate the differential term of ∇_t^2, we obtain

$$k^2 = \frac{k_a^2\int_a E_a^* E_a \, dS \pm k_b^2 \frac{1}{n_a^2}\int_a E_a^* E_b \, dS}{\int_a E_a^* E_a \, dS \pm \int_a E_a^* E_b \, dS} \qquad (2)$$

It is worth noting that these eigenvalues depend on a convolution of the individual NW modes, $\alpha = \int_a E_a^* E_b \, dS / \int_a E_a^* E_a \, dS$. Physically, the parameter α reflects the coupling strength of the leaky mode fields of the neighboring NWs. Equation 2 accurately predicts the locations of (leaky mode) scattering resonances for a wide range of NW diameters and wavelengths of interest. Intuitively, the strongest coupling is expected to occur for the more extended, low-order modes of similar parity. For this reason, we only consider intramode coupling here (i.e., the coupling between modes with identical mode numbers: k_a =

dx.doi.org/10.1021/nl1040429 |Nano Lett. 2011, 11, 1463–1468

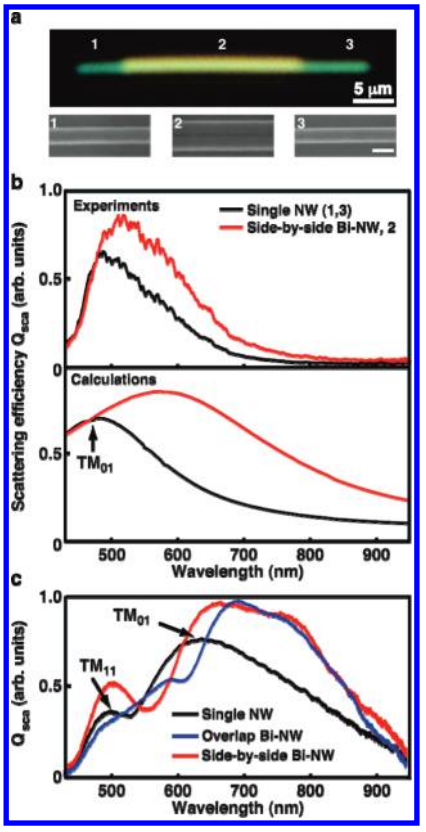

Figure 2. Images and light scattering spectra of binanowire structures. (a) (Upper) True-color darkfield optical image of a bi-NW structure consisting of two silicon NWs with similar diameter of around 35 nm. (Lower) Scanning electron microscopy (SEM) images of the two sections in which the NWs are separated (left and right) and the central section in which the NWs lie side-by-side (middle). The scale bar is 50 nm. (b) Measured (upper) and calculated (lower) light scattering spectra obtained from the different sections of the bi-NW structure under illumination with transverse magnetic (TM) polarized light. The vertical axis shows the scattering efficiency, which is defined as the scattering cross section of the NW normalized by the geometrical cross section. The peak is labeled by the leaky mode resonance (LMR) that gives rise to the strong scattering in this wavelength range (TM_{01}). The calculations are based on the Lorentz−Mie formalism (for single nanowires) and an analytical model developed by Oloafe (for bi-NWs) as discussed in the text. (c) Light scattering spectra for TM-polarized incidence collected from the different sections of a bi-NW structure consisting of two 80 nm diameter silicon NWs, including the sections where the NWs are in the side-by-side configuration (red), the overlap configuration (blue), or by themselves (black). The LMRs associated with the two peaks of the single NW spectrum are labeled as shown. SEM images of the bi-NWs are given in the Supporting Information.

k_b). Under this assumption, eq 2 can be simplified to

$$k^2 = k_a^2\left[1 - \frac{(n_a^2 - 1)\alpha}{n_a^2(1+\alpha)}\right] \quad \text{or} \quad k^2 = k_a^2\left[1 + \frac{(n_a^2 - 1)\alpha}{n_a^2(1-\alpha)}\right] \tag{3}$$

This equation provides the eigenvalues (i.e., resonant frequencies) of the bi-NW system, and we will show that it accurately predicts the frequency shifts and peak-splitting effects observed in the experimental scattering spectra of coupled NWs (Figure 2b,c).

Table 1. Mode Profiles (intensity), Overlap Parameters, and Eigenvalues of the Leaky Resonant Modes of Individual and Coupled NWs[a]

	Single *kr*	Coupling α	Symmetric *kr*	Asymmetric *kr*
TM_{01}	0.83-0.39i	0.72-0.32i	0.62-0.35i	1.36-0.03i
TM_{11}	2.29-0.20i	-0.24+0.16i	2.54-0.47i	2.08-0.07i
TM_{11}		0.20+0.13i	2.09-0.28i	2.53-0.04i
TM_{21}	3.64-0.24i	0.09+0.01i	3.53-0.09i	3.85-0.07i
TM_{21}		-0.14+0.02i	3.95-0.12i	3.46-0.05i

[a] Similar results can be obtained for TE-polarized modes and these are given in the Supporting Information.

Before we analyze peak shifts and peak splitting in our experimental data, it is helpful to explore the wide range of NW coupling effects that can occur with exact calculations of the spectral scattering efficiency. Figure 1a shows a schematic of our typical samples consisting of two parallel semiconductor NWs that are of similar radius *r* and separated by a distance *d*. We start by considering a representative case in which two touching NWs are illuminated in side-by-side and overlap configurations (see inset to Figure 1b). To bring out the essential physics (and avoid complicated effects from materials dispersion), we artificially set the refractive index of the NWs to a constant value of $n = 3.5$; this value is representative of a high index semiconductor. The calculated scattering spectra of the individual and different bi-NW structures are shown in Figure 1b. The calculations are based on the Lorentz−Mie formalism[22] (for single nanowires) and an analytical model developed by Oloafe[23](for bi-NWs). In this figure, the scattering efficiencies are plotted as a function of a normalized parameter nk_0r or kr, where k_0 is the magnitude of the incident wavevector in free space. The bi-NW spectra (red) exhibit significant differences as compared to the individual NW spectrum (black). To identify what changes are due to coupling-induced peak shifts or peak splitting, we next identify the predicted locations of scattering resonances. The location of the LMRs of individual NWs as obtained previously[16] is indicated with black tick marks (Figure 1b). Overall good agreement is found between the calculated peaks in the scattering spectra and the spectral locations of the LMRs. In the depicted size range we can observe features related to the TM_{01}, TM_{11}, and TM_{21} LMRs. Here, we take TM modes to have the magnetic field normal to the NW axis. The first subscript is an azimuthal mode number indicating the effective number of wavelengths around the wire circumference and the second one is a radial order number describing the number of radial field maxima within the NW core.[16] With some approximation, we have taken the real part of these complex eigenvalues that are listed in Table 1 as a predictor for the calculated peak positions. It should be noted that leaky modes by definition have a nonzero imaginary part of the wavenumber, which is largest for very leaky, small-diameter NWs.

The resonance locations of the coupled system predicted by eq 3 are indicated with red ticks. The field plots of the various bonding and antibonding modes are shown in Table 1, together

dx.doi.org/10.1021/nl1040429 |*Nano Lett.* 2011, 11, 1463–1468

with their complex eigenvalues. The bonding(/antibonding) modes tend to have higher (/lower) fields between the NWs, similar to what is seen in molecular systems. It is worth noting that some antibonding and bonding modes with the same azimuthal mode number possess almost degenerate eigenvalues. As a result, their resonance locations (red ticks) cannot be distinguished in Figure 1b. All the peaks in the bi-NW spectra nicely match up with one of the predicted locations of a coupled LMR. Whereas the presented CMT formulation can predict the eigenvalues associated with each of the coupled leaky modes, it does not predict whether a specific coupled mode can be excited to generate observable features in a scattering spectrum. This depends on the illumination conditions and symmetry of the system. For example, we can find that in Figure 1b the antisymmetric TM_{01} coupled leaky mode (kr = 1.2) is present in the spectrum of the overlap configuration but not in the side-by-side configuration. It is clear that the symmetry of the system dictates certain selection rules for plane wave excitation, which has been noted before for the coupling of microspheres and can be derived by applying the reciprocity theorem.[6] In general, the overlap configuration allows excitation of more coupled modes.[6]

With establishment of this theoretical model, we proceed with an experimental investigation of coupled LMRs in bi-NW structures under various excitation conditions. Figure 2a shows a darkfield microscopy image and three scanning electron microscopy (SEM) images taken from different regions of a bi-NW structure consisting of two NWs, which are approximately 35 nm in diameter cast on silicon substrates with a layer of 300 nm thick thermally grown silicon oxide (see Methods for the experimental details on the NW synthesis via the vapor−liquid−solid (VLS) technique). The middle section appears yellow in the darkfield image and corresponds to a region in which the NWs are in very close proximity (shown as section 2 and again referred to as the "side-by-side" configuration). The two end sections appear green and correspond to regions where the NWs are well-separated (sections 1 and 3 are referred to as "single" NW sections). Our confocal microscope allows light scattering signals to be collected from each of these distinct areas in separate measurements (see Methods section). The light scattering spectra collected from the different areas are presented in Figure 2b. The spectra taken from the different individual NW sections are very similar (as expected based on their similar diameter) and only one of the spectra is shown (black curve). This spectrum shows one broad peak with a maximum near 490 nm. The scattering spectrum taken from the side-by-side bi-NW region (section 2) differs from the single NW spectrum. Most notably, the 490 nm peak (TM_{01}) of the single NW red shifts to around 530 nm, and this spectral shift is consistent with the more yellow appearance in the darkfield microscopy image.

More complex behavior can be seen for bi-NW configurations consisting of larger diameter wires. For example, Figure 2c shows the scattering spectra taken from 80 nm diameter NW and bi-NW structures. The two bi-NW spectra are appropriate for the cases where the NWs lay side-by-side or on top of each other (termed the "overlap" configuration). It can be seen that this larger diameter NW gives rise to two scattering resonances (500 nm TM_{01} and 620 nm TM_{11}) in the spectral range from 450 to 950 nm. The spectrum taken from the side-by-side bi-NW system again shows a red shift for the TM_{01} peak and no significant shift is observed for the TM_{11} peak. The spectrum associated with the overlap configuration shows that the individual NW TM_{01} peak has split into two new ones appearing at 590 and 690 nm, respectively.

The experimentally observed peak positions and spectral shifts that occur upon coupling are in good qualitative agreement with the calculated spectra. For example, the observed red shift of the TM_{01} peak in side-by-side NW spectra taken from the 35 nm diameter wires (Figure 2b upper) correlate well with the calculated scattering spectra (Figure 2b lower). The shift is also consistent with our earlier calculations presented in Figure 1b, but this time we plotted the calculated scattering efficiency as a function of wavelength for easy comparison to the experimental spectra. It can also be seen in experiments (Figure 2c) and theory (Figure 1b) that the position of the TM_{11} peak is less sensitive to coupling effects than the TM_{01} peak. This is expected because the TM_{11} mode is more confined and the resulting mode overlap is reduced (i.e., a smaller α). The predicted configuration-dependent excitation of coupled LMRs is also observed in the experiments shown in Figure 2c. In the calculations (Figure 1b) and experiments, the TM_{01} peak was observed to red shift in side-by-side NW spectra while it split into two new peaks in the overlap configuration.

The presented CMT formulation provides valuable understanding on some of the more subtle optical coupling features of nanoresonators that are distinct from microresonators. For example, the resonant modes of high-confinement microresonators split symmetrically. This means that upon coupling, the antisymmetric modes blue shift as much as the symmetric modes red shift.[6,24] In contrast, Figure 1b predicts substantially asymmetric splitting behavior for the lowest-order coupled leaky modes of nanoresonators. From eq 3 it can be seen that an asymmetrical splitting can result for sufficiently large α values; these can be achieved for low-order leaky modes in pairs of small diameter wires. In such cases the poor confinement of the mode inside the NW results in strong coupling. Table 1 and Figure 1b show that this type of asymmetry tends to be smaller for higher-order, more confined modes.

As the nature and strength of the coupling between deep-subwavelength, nanoscale resonators can intuitively be very different from more confined micrometerscale systems, we continue with a systematic experimental study of this physical quantity. We show that eq 3 can quantitatively predict the unique oscillatory dependence of the coupling on the interspacing between NWs and its substantial strength. In particular, we examined the light scattering spectra (Figure 3a) from a series of bi-NW structures with varying interspacings. NW pairs with a square cross section that measured 170 nm along the sides were fabricated using standard polycrystalline silicon thin-film deposition, lithographic patterning, and dry etching (Figure 3b). As the scattering behavior of low-order leaky mode resonances are qualitatively similar for distinct geometrical cross sections of the nanowire (circular, square, triangular),[25] it is expected that they also exhibit a similar coupling behavior. For this reason the square NWs provide a valuable system for study in which the critical dimensions can be controlled more effectively by lithographic means. Figure 3a shows that the single NW scattering spectrum exhibits a number of distinct peaks (curve 8). All of the observed peaks are reproduced in full-field electromagnetic simulations (see Figure S3, Supporting Information). In this paper, we will direct our attention to the scattering peak near 750 nm, whose origin and dipolar field distribution are similar to that of the TM_{11} mode of a cylindrical NW. As the spacing between the NWs is reduced from 5 μm to 280 nm, a significant

dx.doi.org/10.1021/nl1040429 |Nano Lett. 2011, 11, 1463–1468

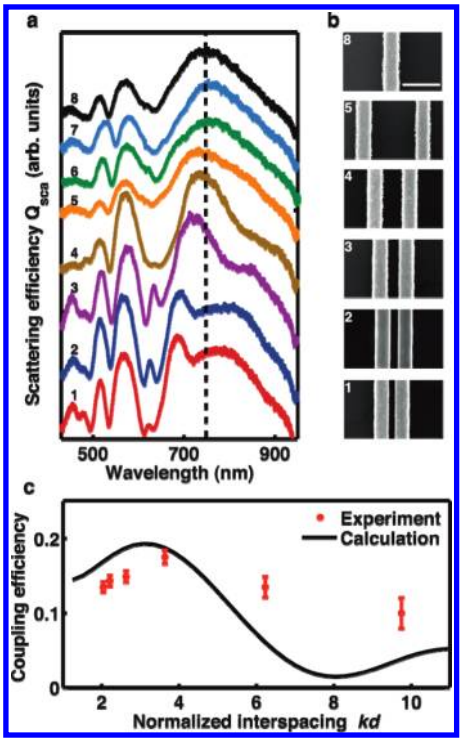

Figure 3. Dependence of the optical coupling strength on the inter-nanowire spacing. (a) Light scattering spectra of bi-NW structures that consist of two square NWs measuring 170 nm on the side. The spectra are shown for NW interspacings of (1) 280 nm, (2) 300 nm, (3) 350 nm, (4) 460 nm, (5) 780 nm, (6) 1300 nm, and (7) 5 μm. The scattering spectrum of a single 170 nm size NW is given for comparison (curve 8). The bi-NWs were generated by standard polysilicon thin film deposition followed by e-beam lithography and dry etching. (b) SEM images of representative bi-NWs are shown as labeled. (c) Comparison between the measured coupling efficiency of the fabricated, square cross-section wires (red dot) and calculated coupling efficiencies for a pair of cylindrical wires (black solid line). The coupling efficiency was related to the degree of peak splitting in the spectral broad spectral feature near 800 nm. The peak-splitting was analyzed by a peak-fitting procedure that assumed a Gaussian profile for all resonances. The error bars quantify our ability to identify the individual peak positions.

splitting can again be observed. This peak splitting is nicely reproduced by full-field electromagnetic simulations (see Figure S3, Supporting Information). In order to assess the coupling strength from our measurements, we analyze the strength of the inter-NW coupling by defining a coupling efficiency as $\gamma = (1/\lambda_1 - 1/\lambda_2)/(1/\lambda_0)$ where λ_1, λ_2 are the wavelengths of the split peaks in bi-NWs and λ_0 is the peak position of the single NW(λ_0 = 750 nm here). By introducing this phenomenological coupling efficiency, we can compare the experimental observations to the theoretical predictions from eq 3 for circular bi-NWs whose diameter is the same as the width of the square NWs used in the experiments. Figure 3c shows the experimental and calculated values of the coupling efficiency γ as a function of a normalized interspacing kd, where d is the center-to-center distance of the two NWs and $k = 2\pi/\lambda_0$. We can see that the theory predicts the right order of magnitude for the coupling strength and reasonable qualitative agreement is obtained. As eq 3 was derived for circular cross section NWs in a uniform medium and the experiments were performed on square cross section wires on a substrate, the agreement between experiments and theory is not expected to be exact. However, the comparison is of value as the simple theoretical model on the idealized cylindrical NW geometry nicely highlights the underlying physics. The values of γ can reach up to 0.2, indicative of a coupling that is about 2 orders of magnitude stronger than typically seen in microscale resonators.[6,24] The theory also predicts a nonmonotonic dependence in the decay of the coupling strength with increasing inter-NW spacing. This unique spatial dependence is reminiscent of the nature of the leaky modes' fields outside the nanowire that is mathematically in a form of a Hankel function that exhibits oscillations on the wavelength scale.[21] Interestingly, both experiment and theory show that the maximum coupling appears at a specific, nonzero value of kd. In experiments on high confinement microresonators, the coupling is seen to always monotonically decay as a function of the interspacing. This is understandable because the effects of the wavelength scale oscillations in the Hankel function on the coupling are averaged out in systems that are large compared to the wavelength.

The experimental measurements and the proposed theoretical model clearly reveal the nature of the leaky mode coupling between semiconductor nanowires. Whereas the guided mode coupling of semiconductor nanowires has been the topic of much research,[3,14,17,18] this is the first report on the leaky mode coupling of two deep subwavelength nanowires at optical frequency. Interestingly, the presented results reveal that this coupling can be orders of magnitude stronger than that in coupled microresonators and enables effective optical engineering of the resonant behavior of coupled systems. As the optical coupling is not unique to the wire geometry, similar engineering of optical resonances can be achieved in high index semiconductor nanoparticles of different shape. The ability of engineer optical resonances in semiconductor nanostructures directly impacts topical physics research, including metamaterials and nanoscale antenna design, structural EIT, light trapping in solar cells, photodetectors, and biosensors. It also nicely complements ongoing efforts to study the coupling of metallic nanostructures that also can serve as effective antenna through their ability to support surface plasmon excitations.[29] The presented coupled mode theory quantifies the interaction between leaky modes of the nanowires and provides an intuitive vantage point from which to understand and engineer optically the coupled nanoresonators. As a result, the demonstrated efficient optical coupling of semiconductor nanostructures opens up an entirely new avenue to engineer light−matter interaction and to route and actively manipulate light at the nanoscale.

Methods. The light scattering measurements were carried out on a confocal optical microscope with white light focused onto a variety of closely spaced silicon NWs (SiNWs) through a Nikon 100× microscope objective. The elastically scattered light from the SiNWs was collected in a backscattering configuration and analyzed with a spectrometer.[26] One set of SiNWs were grown via gold colloid-catalyzed chemical vapor deposition,[27] sonicated in isoproponol solution, and finally dispersed onto Si substrates with a 300 nm thick thermally grown oxide. Such NWs present an almost ideal model system because of their well-defined morphology and crystal structure.[27] Upon inspection in a scanning electron microscope, it was found that many of the SiNWs were well separated, whereas some happened to find themselves in close proximity to each other. A second set of bi-NW structures with varying interspacings were generated using standard polycrystalline silicon thin-film deposition, lithographic patterning, and dry etching.

dx.doi.org/10.1021/nl1040429 |*Nano Lett.* 2011, 11, 1463–1468

■ ASSOCIATED CONTENT

Supporting Information. Figures showing SEM image of a bi-nanowire, correlation of the light scattering spectra of bi-nanowire structures, and measured and simulated light scattering spectra of a single, square nanowire and bi-nanowire. This material is available free of charge via the Internet at http://pubs.acs.org.

■ AUTHOR INFORMATION

Corresponding Author
*E-mail: brongersma@stanford.edu.

■ ACKNOWLEDGMENT

This material is based upon work supported as part of the Center on Nanostructuring for Efficient Energy Conversion (CNEEC) at Stanford University, an Energy Frontier Research Center funded by the U.S. Department of Energy, Office of Science, Office of Basic Energy Sciences under Award Number DE-SC0001060.

■ REFERENCES

(1) Vahala, K. J. Optical Microcavities. *Nature* **2003**, *424*, 839–846.
(2) Prodan, E.; Radloff, C.; Halas, N. J.; Nordlander, P. A hybridization model for the plasmon response of complex nanostructures. *Science* **2003**, *302*, 419–422.
(3) Povinelli, M. L.; et al. Evanescent-wave bonding between optical waveguides. *Opt. Lett.* **2005**, *30*, 3042–3044.
(4) Wiederhecker, G. S.; Chen, L.; Gondarenko, A.; Lipson, M. Controlling photonic structures using optical forces. *Nature* **2009**, *462*, 633–636.
(5) Villeneuve, P. R.; Fan, S.; Joannopoulos, J. D. Microcavities in photonic crystals: mode symmetry, tunability and coupling efficiency. *Phys. Rev. B* **1996**, *54*, 7837–7842.
(6) Mukaiyama, T.; Takeda, K.; Miyazaki, H.; Jimba, Y.; Kuwata-Gonokami, M. Tight-binding photonic molecule modes of resonant bisheres. *Phys. Rev. Lett.* **1999**, *82*, 4623–4626.
(7) Bayer, M.; et al. Optical demonstration of a crystal band structure formation. *Phys. Rev. Lett.* **1999**, *83*, 5374–5377.
(8) Lin, Q.; Rosenberg, J.; Jiang, X.; Vahala, K. J.; Painter, O. Mechanical oscillation of cooling actuated by the optical gradient force. *Phys. Rev. Lett.* **2009**, *103*, 103601.
(9) Yariv, A.; Xu, Y.; Lee, R. K.; Scherer, A. Coupled-resonator optical waveguide: a proposal and analysis. *Opt. Lett.* **1999**, *24*, 711–713.
(10) Little, B. E.; Chu, S. T.; Haus, H. A.; Foresi, J.; Laine, J. P. Microring resonator channel dropping filters. *J. Lightwave Technol.* **1997**, *15*, 998–1005.
(11) Xu, Q.; et al. Experimental realization of an on-chip all-optical analogue to electromagnetically induced transparency. *Phys. Rev. Lett.* **2006**, *96*, 123901.
(12) Schmidt, C.; et al. Observation of optical coupling in microdisk resonators. *Phys. Rev. A* **2009**, *80*, 043841.
(13) Xifre-perez, E.; Abajo, F. J. G. d.; Fenollosa, R.; Meseguer, F. Photonic binding in silicon-colloid microcavities. *Phys. Rev. Lett.* **2009**, *103*, 103902.
(14) Li, M.; Pernice, W. H. P.; Tang, H. X. Tunable bipolar optical interactions betwen guided lightwaves. *Nat. Photonics* **2009**, *3*, 464–468.
(15) Fan, S.; et al. Guided and defect modes in periodic dielectric waveguides. *J. Opt. Soc. Am. B* **1995**, *12*, 1267–1272.
(16) Cao, L.; et al. Engineering light absorption in semiconductor nanowire devices. *Nat. Mater.* **2009**, *8*, 643–647.
(17) Roels, J.; et al. Tunable optical forces between nanophotonic waveguides. *Nat. Nanotechnol.* **2009**, *4*, 510–513.
(18) Eichenfield, M.; Camacho, R.; Chan, J.; Vahala, K. J.; Painter, O. A picogram- and nanometre-scale photonic-crystal optomechanical cavity. *Nature* **2009**, *459*, 550–555.
(19) Cao, L.; Nabet, B.; Spanier, J. E. Enhanced Raman scattering from individual semiconductor nanocones and nanowires. *Phys. Rev. Lett.* **2006**, *96*, 157402.
(20) Cao, L.; Park, J.-S.; Fan, P.; Clemens, B. M.; Brongersma, M. L. *Nano Lett.* **2010**, *10*, 1229–1233.
(21) Haus, H. A. *Waves and fields in optoelectronics*; Prentice-Hall: Englewood Cliffs, 1984.
(22) Snyder, A. W. *Optical Waveguide Theory*; Springer: Berlin, 1983.
(23) Bohren, C. F.; Huffman, D. R. *Absorption and Scattering of Light by Small Particles*; John Wiley & Sons, Inc.: New York, 1998.
(24) Olaofe, G. O. Scattering by two cylinders. *Radio Sci.* **1970**, *5*, 1351–1360.
(25) Khitrova, G.; Gibbs, H. M.; Jahnke, F.; Kira, M.; Koch, S. W. Nonlinear optics of normal-mode-coupling semiconductor microcavities. *Rev. Mod. Phys.* **1999**, *71*, 1591–1639.
(26) Cao, L.; Fan, P.; Vasudev, A. P.; White, J. S.; Yu, Z.; Cai, W.; Schuller, J. A.; Fan, S.; Brongersma, M. L. Semiconductor nanowire optical antenna solar absorbers. *Nano Lett.* **2010**, *10*, 439–445.
(27) Cao, L.; Fan, P.; Barnard, E.; Brown, A.; Brongersma, M. L. Tuning the color of silicon nanostructures. *Nano Lett.* **2010**, *10*, 2649–2654.
(28) Cui, Y.; Lauhon, L. J.; Gudiksen, M. S.; Wang, J.; Lieber, C. M. Diameter-controlled synthesis of single-crystal silicon nanowires. *Appl. Phys. Lett.* **2001**, *78*, 2214.
(29) Prodan, E.; Radloff, C.; Halas, N. J.; Nordlander, P. A Hybridization Model for the Plasmon Response of Complex Nanostructures. *Science* **2003**, *17*, 419–422.